

# An Innovative Trapezium Normalization for Iris Recognition Systems

Mahboubeh Shamsi<sup>1</sup> and Abdolreza Rasouli<sup>2+</sup>

Islamic Azad University, Bardsir, Kerman, Iran

**Abstract.** Iris normalisation and feature extraction are two last stages of iris processing in iris recognition systems. In normalisation step, the segmented iris disk is transformed to a strip. The most iris recognition systems are employed rectangular strip normalisation. In this paper, the problems such as repeating or losing information in rectangular normalisation method are investigated. The new trapezium normalisation also has been developed to enhance the normalisation stage. The 2D Gabor filter is employed to extract the iris features from the trapezium normalised image. The impacts of trapezium normalisation versus rectangular normalisation on extracted features are discussed. The result shows the significant improve in case of CASIA iris repository.

**Keywords:** Iris recognition, Normalization, Trapezium Normalization, Segmentation.

## 1. Introduction

In the normalisation step, the iris region is transformed to a strip to extract features. In a standard condition, an acceptable normalisation technique should lead to different strip image for different irises and produce same strip image for same iris. In some cases, the centre of pupil and iris are not coincident, and there is small incongruent between them. This incongruence is a big challenge in ellipse shaped iris images. Briefly, the main process of the normalisation step is remapping the image from Cartesian coordinate to polar coordinate.

After normalisation, the unique features are extracted from a normalised image. In feature extraction, the normalised image is encoded to significant integers or binary code. Most iris recognition systems use band pass filters like wavelets or Fourier series to produce a desirable feature codes. These irises codes are compared to identify that they were produced from the same irises or different irises. A good technique should produce same code from same irises and different code from different irises. In this paper, a Trapezium normalisation method is developed to reduce the repetition or losing important features.

## 2. Background and Related Work

When the iris region is separated, next step is normalising the iris image. Each researcher used different method to convert the iris image points from Cartesian to polar coordinate. But in all techniques, it was noted that the different levels of illumination affect on the contrast or expanding the area of iris and pupil. Other cases such as the distance image, motion and angle of camera and position of head/eye can be influential on the dimensional image for normalisation [1]. While the centre of the pupil and iris is not consistent, it affects on the iris disk and radius. Here some methods will be examined.

The Daugman's algorithm [2,3,4,5,6] was supposed to use rubber sheet model. The rubber sheet model converts each point in Cartesian coordinate to polar coordinate. So Daugman applied rubber sheet model to change each pixel coordinate in iris region from Cartesian to polar. First, he set the centre of the pupil with a reference point. Then he put the radial vectors through the iris area. Daugman picked out some points that were in line to recognise and arrange in rays resolution, while also using the number of points that were

---

<sup>+1</sup> mahboubeshamsi@yahoo.com, <sup>2</sup> rs.reza@gmail.com

around the iris area to angular resolution [7]. Daugman tried to remap  $(x, y)$  from Cartesian coordinate to  $(r, \theta)$  in polar coordinate. The Daugman's method is formulated as below:

$$I(x(r, \theta), y(r, \theta)) \rightarrow I(r, \theta): \begin{cases} x(r, \theta) = (1-r)x_p(\theta) + rx_i(\theta) \\ y(r, \theta) = (1-r)y_p(\theta) + ry_i(\theta) \end{cases} \quad (1)$$

Where  $I(x, y)$  is the image intensity function,  $(x, y)$  are the Cartesian coordinate,  $(r, \theta)$  are the normalised polar coordinate,  $x_p, y_p$  are the coordinate of the pupil contour pixel along the direction  $\theta$  and  $x_i, y_i$  are the coordinate of the iris contour pixel along the direction of  $\theta$ .

Another normalisation method implemented by Wildes et al. [8,9,10,11]. In this system,  $I_a(x, y)$  is a image which is acquired and  $I_d(x, y)$  is a selected image from the repository. Then these two parameters must align together. This system needed more time because each image must pass minimisation procedure repetitiously.

The system by Boles [12] tried to find constant diameter and then change the size of image by it. He did it to compare two images in which one of them was a reference image. In this technique, the first two iris areas match together approximately and if the difference is small, second normalisation process will run. The intensity values of iris region points stores along the virtual concentric circles only if the origin is at the pupil's centre. It is a weakness in Boles system, on how rotational invariance is obtained [7].

Finally, each scholar used one of the above methods to normalise the iris region and then they used different filters to extract the characteristics and feature from the iris area [3,13,14,15,16].

### 3. Discrepancies of the Rectangular Normalisation

In any disk, the radius of inner circle is lesser than outer circle. It means that the exact normalised shape of the disk is not rectangle strip. If the height of normalised image is  $r_{iris} - r_{pupil}$ , two approaches could be imagined for the width of normalised image in direction  $\theta$ . The first approach is choosing a fix height for all iris images as 360 pixels for every degree around the circle. In this approach, some pixels of the original image will lose in normalised image. This fact is shown in Fig.1.a While the  $\theta$  sweeps the iris area, only the pixel at the  $\theta$  direction is normalised and all pixels among the two degrees are vanished. These pixels are hachured.

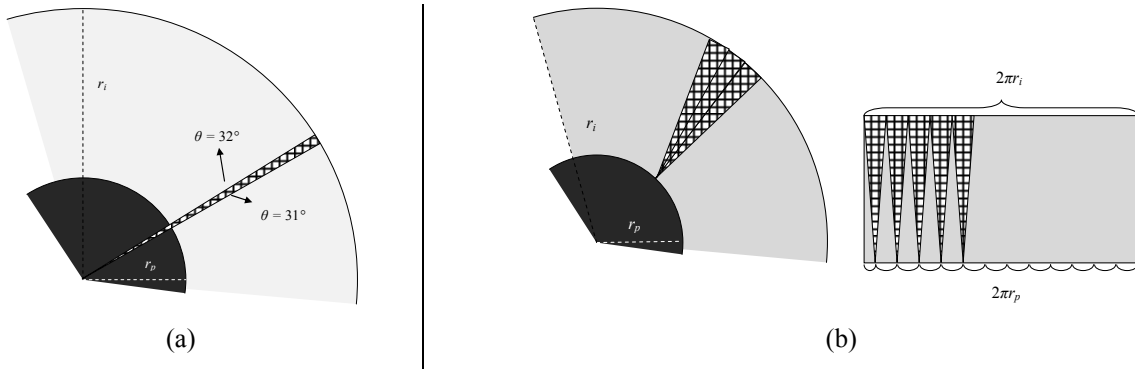


Fig. 1. a) Loosing some pixel between two consecutive degree – b) Repetition of pixels in Normalisation

The second approach is sweeping the disk with the maximum possible value. The maximum circular pixel in disk belongs to the iris boundary and equals to circumference of iris as  $2\pi r_i$ . In this approach, the width of the normalised image is  $2\pi r_i$  and  $\theta$  will change in gradient metric in the range  $0, 2\pi$  instead of  $0, 360$ . Contrary to previous approach, this time, some pixels are repeated in the normalised image. This problem happened due to lower value of pupil radius related to iris radius. In fact, because  $r_{pupil} < r_{iris}$ , thereupon the pupil circumference is less than iris circumference or  $2\pi r_p < 2\pi r_i$ . In order to compensate the lack of pixels, the approach has to fill the empty space with repetition of pixels. Fig.1.b shows this problem. Most of the researchers use the rectangular strip normalisation, because it is easier to compute and implement.

*Trapezium View.* In order to solve the problems occurred in rectangular strip normalisation, a trapezium view is proposed. In this method, each pixel inside the iris disk is mapped to one and only one pixel in the

normalised image. The method is based on a dynamic width for a normalised strip, so the strip width become less while the  $r$  is closed to pupil and inverse. The trapezium view is shown in Fig.2.

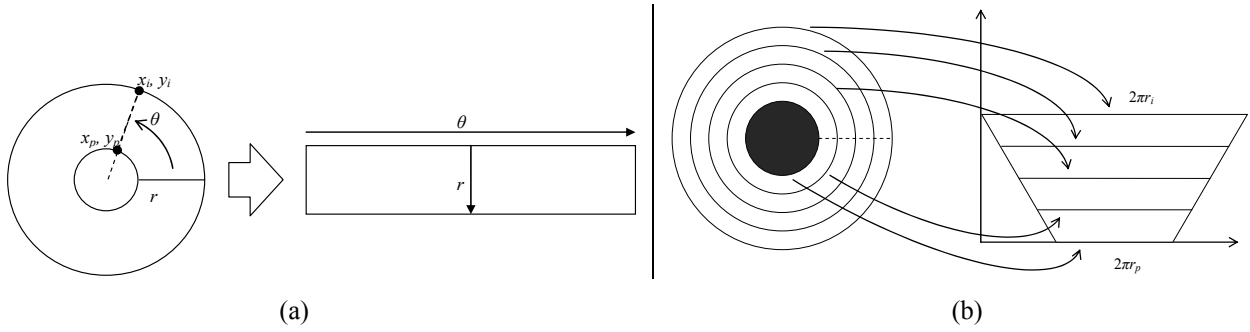


Fig. 2. a) Rectangular Daugman's Rubber Sheet Model – b) Trapezium view of Normalisation process

If the iris region is circular, then the normalised image is exactly trapeze, but if the iris be ellipse, then the normalised image is a skewed trapeze. The trapezium strip could be compute as follows;

$$\begin{aligned}
 I_{norm}(r, \theta) &= I(x, y) \Rightarrow r = \sqrt{(x - x_0)^2 + (y - y_0)^2}, r_p \leq r \leq r_i \\
 \theta &= \arctan\left(\frac{y - y_0}{x - x_0}\right) \Rightarrow \theta' = \theta.r + \left(\frac{2\pi r_i - 2\pi r}{2}\right), 0 \leq \theta \leq 2\pi
 \end{aligned} \tag{2}$$

#### 4. Feature Extraction

Iris feature extraction is a process of encoding the normalised image to the digitised code. This code is used to compare other iris codes for best matching state. The Gabor filter is chosen to extract textural features because it can effectively extract the frequency component of the iris. Daugman convolutes the 2D Gabor filter with the iris normalised image as

$$h_{(Re, Im)} = \text{sgn}_{(Re, Im)} \iint_{\rho \phi} \left( I(\rho, \phi) e^{-j\omega(\theta_0 - \phi)} e^{\frac{-(r_0 - \rho)^2}{\alpha^2}} e^{\frac{-(\theta_0 - \phi)^2}{\beta^2}} \right) \rho d\rho d\phi \tag{3}$$

Where  $I(\rho, \phi)$  is the normalised image in polar coordinate.  $\alpha$  and  $\beta$  are the multi scale 2D wavelet size parameters and  $\omega$  is the wavelet frequency.  $(r_0, \theta_0)$  are the polar coordinates of each region of iris that the features are computed.

In order to match iris codes, the hamming distance is employed for matching process due to its widely usage in most systems. Suppose that there are two iris codes  $A, B$ ; then the hamming distance as Daugman [4] defines is:

$$HD = \frac{\|(\text{Code}_A \otimes \text{Code}_B) \cap \text{Mask}_A \cap \text{Mask}_B\|}{\|\text{Mask}_A \cap \text{Mask}_B\|} \tag{4}$$

#### 5. Trapezium Normalisation vs. Rectangular Normalisation

For this experiment, 50 individuals, each individual 2 eyes, totally 100 eyes is selected from CASIA iris repository. A total of 4950 comparisons were done over these eyes. A 128 bit iris code is proposed for this experiment. Each normalised image is divided into  $8 \times 8$  rectangle, totally 64 rectangles. Each rectangle produces two bit according to its convolution with real and imaginary Gabor filter matrixes. In the first phase, features are extracted from rectangular strip normalised image provided by rubber sheet model. In the second phase, feature extraction process with same parameters is applied on trapezium normalised images.

The intraclass and interclass distribution obtained from rectangular normalised images are shown in Fig.3.a. The intraclass hamming distance varies from 0.22 to 0.40 and interclass hamming distance varies from 0.34 to 0.70. The intraclass and interclass distribution obtained from trapezium normalised images are shown in Fig.3.b. In this case, the intraclass hamming distance varies from 0.14 to 0.33 and interclass hamming distance varies from 0.30 to 0.70.

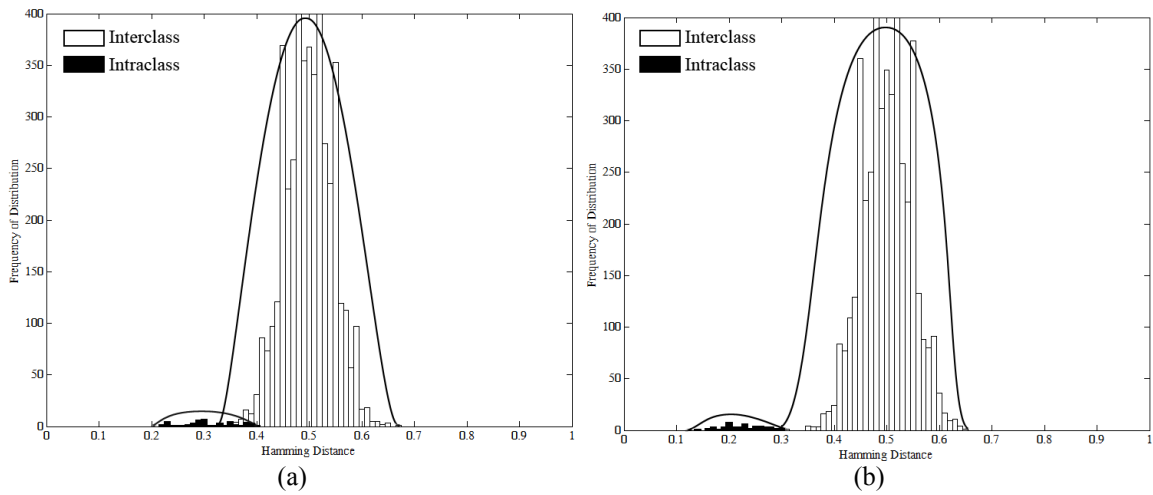


Fig. 3. a) The CASIA intraclass and interclass hamming distance distribution of rectangular strip Normalisation – b) The CASIA intraclass and interclass hamming distance distribution of trapezium Normalisation

With regards to the experimental results, two enhancements are observed. The initial improvement is that the intersection between interclass and intraclass in trapezium normalisation becomes less related to the rectangular normalisation. The intersection in second phase occurs in the range between 0.3 and 0.33, whereas in first phase, this intersection occurs in the range of 0.34 to 0.40. The second improvement is that in the trapezium normalisation the frequency is distributed lower along the hamming distance axis. In fact, the iris codes are more similar than the first phase, rectangular normalisation. The results shows that, the mathematical demonstration about non repetition and non losing information in trapezium normalisation has positive impact on the feature extraction stage.

## 6. Conclusions

The False Acceptance Rate and False Rejection Rate are computed for trapezium over the range between 0.2 and 0.5. The results are shown in Fig.4.a. The FRR rate is around 68%, while the threshold is 0.2, because 68% of the intraclass hamming distance are between 0.2 and 0.3 and they reject, whereas they should accept. The FAR rate is 0, because no interclass hamming distance is less than 0.2, so no one accepts. Inverse while the threshold is 0.5, the FRR rate is 0, because all intraclass hamming distance are less than 0.5 and there is not a false rejection. While that FAR rate is increased to 53%, it means that 53% of interclass hamming distances are less than 0.5 and they accept wrongly. The supremum value of intraclass hamming distances is 0.33 and so the FRR tends to 0 after 0.3. Inverse the infimum value of interclass hamming distances is the 0.3, so before the threshold value equal to 0.3, the FAR rate is 0.

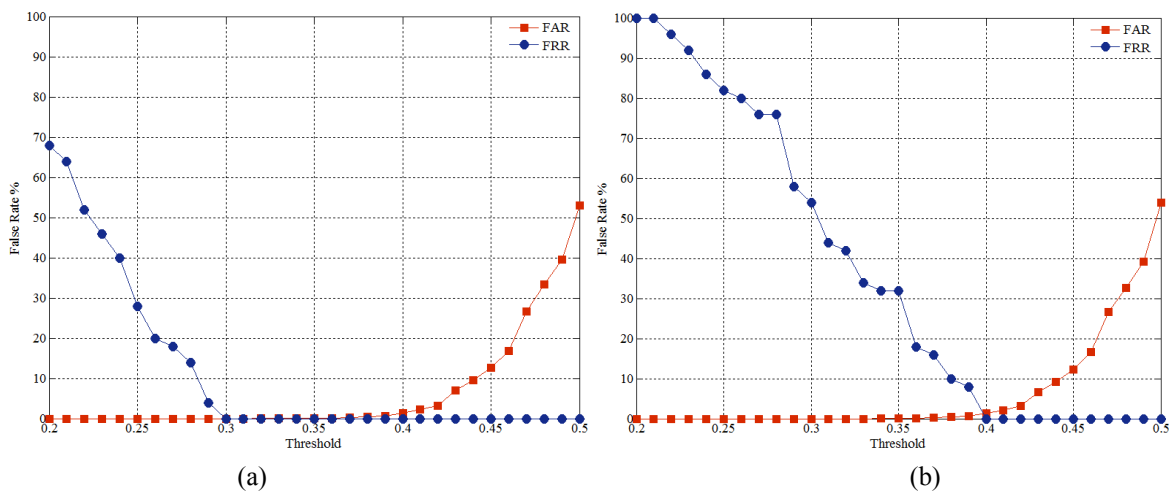


Fig. 4. a) The FAR and FRR for Trapezium Normalisation – b) The FAR and FRR for Rectangular Normalisation

Same as above, the False Acceptance Rate and False Rejection Rate are computed for rectangular over the range between 0.2 and 0.5. The results are shown in Fig.4.b. The infimum value of interclass hamming distances is the 0.34, so the FAR rate is 0 before the threshold value of 0.34. The supremum value of

intraclass hamming distances is 0.4 and so the FRR tends to 0 after 0.4. Against the trapezium the FRR rate is 100%, while the threshold is 0.2 and it means that 100% of the intraclass hamming distance are more than 0.2, so they rejected. The lower value of FRR for trapezium ensures more similarity between iris codes produced in trapezium normalisation related to rectangular normalisation. While the threshold is 0.5, the FAR rate is increased to 55%, it means that 55% of interclass hamming distances are less than 0.5 and they accept wrongly.

The best EER rate for trapezium normalisation as base as the intersection point of FAR and FRR is 0.3, whereas the best EER for rectangular normalisation is 0.4. As we mentioned before, the lower value proves the better performance of the trapezium normalisation. Because in the trapezium normalisation the iris codes for same subject are more similar together than rectangular normalisation. Moreover, high gradient of the FAR and FRR curve in rectangular normalisation related to trapezium normalisation, ensures the increase of error rate.

## 7. References

- [1] J. G. Daugman. How iris recognition works. *Proceedings of 2002 International Conference on Image Processing*. (2002).
- [2] S. Sanderson and J. Erbetta. Authentication for secure environments based on iris scanning technology. *IEE Colloquium on Visual Biometrics*. 8/1-8/7 (2000).
- [3] M. Shamsi, P. B. Saad, S. B. Ibrahim and A. r. Rasouli. Fast Algorithm for Iris Localization Using Daugman Circular Integro Differential Operator. International Conference of Soft Computing and Pattern Recognition, SoCPaR09 (2009).
- [4] J. Daugman and C. Downing. Effect of Severe Image Compression on Iris Recognition Performance. *IEEE Transactions on Information Forensics and Security*. 3 (1), 52-61 (2008).
- [5] J. Daugman. New Methods in Iris Recognition. *IEEE Transactions on Systems, Man, and Cybernetics, Part B: Cybernetics*. 37 (5), 1167-1175 (2007).
- [6] J. G. Daugman, R. Anderson and F. Hao. Combining Crypto with Biometrics Effectively. *IEEE Trans. on Computers*. 55 (9) (2006).
- [7] P. Sinha. *Massachusetts Institute of Technology*. 1992.
- [8] P. R. Wildes. Iris Recognition: An Emerging Biometric Technology. *Proceeding of the IEEE*. 85 (9), 1348 - 1363 (1997).
- [9] C. Fancourt , L. Bogoni, K. Hanna, Y. Guo, R. Wildes, N. Takahashi and U. Jain. Iris recognition at a distance. in *Audio- and Video-Based Biometric Person Authentication, Lecture Notes in Computer Science* (Springer, 2005), Vol. 3546, pp. 1-13.
- [10] T. A. Camus and R. Wildes. Reliable and fast eye finding in closeup images. IEEE 16th Int. Conf. on Pattern Recognition, Quebec, Canada, 389-394 (2004).
- [11] R. Wildes, J. Asmuth, G. Green and S. Hsu. A system for automated iris recognition. Second IEEE Workshop on Applications of Computer Vision, 121 - 128 (2004).
- [12] W. Boles and B. Boashash. A human identification technique using images of the iris and wavelet transform. *IEEE Transactions on Signal Processing*. 46 (4), 1185-1188 (1998).
- [13] M. Shamsi, P. B. Saad, S. B. Ibrahim and A. r. Rasouli. A New Accurate Technique for Iris Boundary Detection. *WSEAS Transactions on Computers*. 9 (1) (2010).
- [14] M. Shamsi and A. R. Rasouli. A Novel Approach for Iris Segmentation and Normalization. Second International Conference on the Applications of Digital Information and Web Technologies (ICADIWT 2009) (2009).
- [15] M. Shamsi, P. B. Saad and A. R. Rasouli. An Advanced Method for Iris Segmentation and Normalization. *International Journal of Web Applications*. 3 (3) (2009).
- [16] M. Shamsi, P. B. Saad, and A. R. Rasouli. Iris Segmentation and Normalization Approach. *Journal of Information Technology (Universiti Teknologi Malaysia)*. 19 (2) (2008).